Doppler shifted cyclotron maser radiation pumped by an asymmetric undulator

I. Shraga, C. Leibovitch, and S. Eckhouse
Applied Physics Department, Ministry of Defense, P. O. Box 2250, Haifa, Israel

Y. Goren[a)]
Department of Physics and Astronomy, Tel Aviv University, Ramat-Aviv, Israel

A. Gover
School of Engineering, Tel-Aviv University, Ramat-Aviv, Israel

(Received 16 August 1984; accepted for publication 7 March 1985)

Super-radiant microwave emission pumped by the second harmonics of an asymmetric undulator has been investigated. Intense emission of TE mode electron cyclotron maser radiation was detected near the cyclotron resonance. It has been shown that an asymmetric undulator can be a suitable tool in producing high-frequency intense microwave radiation without any change in its fundamental period.

During the past decade millimeter and submillimeter high power sources (megawatts to gigawatts) using intense relativistic electron beams have received considerable interest.[1–4] Two classes of electron beam instabilities have been investigated most extensively: (a) the electron cyclotron maser mechanism (ECM) in which the radiation is characterized by the electron gyrofrequency and its harmonics[5,6], (b) the free-electron laser mechanism whose emission frequency is characterized by twice the Doppler up-shift of a given initial frequency. In this letter we present experimental and computer simulation results of Doppler shifted ECM radiation pumped by a rippled magnetic field with an asymmetric periodicity. The asymmetric undulator enables generation of microwave at high harmonics of the period of the rippled field.

A rippled magnetic field is usually an inefficient way of converting translational electron energy into transverse energy, unless its period is close to the cyclotron period. When these two periods coincide one can expect a strong transverse perturbation in the electron trajectories.[7] The field dependence on the radius r and the axial coordinate z can be expressed as follows:

$$B_z(r,z) = B_0\left(1-\alpha+\alpha\sum_{n=1}^{\infty} b_n\, I_0(k_n\, r)\cos(k_n\, z)\right), \tag{1}$$

$$B_r(r,z) = B_0\,\alpha\sum_{n=1}^{\infty} b_n\, I_1(k_n\, r)\sin(k_n\, z), \tag{2}$$

where B_0 is the uniform unperturbed axial magnetic field and α is the rippled field amplitude. b_n is the nth Fourier amplitude of the rippled field, $k_n = nk_0 = n2\pi/L$ as its wave number, and L is the perturbation period. We require that

$$\sum_{n=1}^{\infty} b_n = 1\,. \tag{3}$$

I_0 and I_1 in Eqs. (1) and (2) are the modified Bessel functions of the first kind of orders zero and unity, respectively. We assume a solid cylindrical beam moving parallel to the field. Substituting Eqs. (1) and (2) together with the electron beam self-electric and magnetic fields into the single particle equation of motion one can calculate the amount of axial energy which is converted to transverse energy. The electrons at the edge of the beam will be affected most strongly by the rippled field. Expanding the equation of motion to first order in the rippled field amplitude α and in the radial excursion ρ around the equilibrium radial position R of the electron we obtain the radial electron trajectory equation:

$$\frac{d^2\rho}{dz^2}+\left(\frac{(\Omega_0/\gamma V_\parallel)^2-\omega_{pe}^2}{2\gamma^3 V_\parallel^2}\right)\rho = -\left(\frac{\Omega_0}{\gamma V_\parallel}\right)^2\frac{\alpha}{1-\alpha}\sum_{n=1}^{\infty}\frac{b_n}{k_n}I_1(k_n\,R)\cos(k_n\,z), \tag{4}$$

where $\Omega_0 = eB_0/m_0c$ is the electron cyclotron frequency, $\omega_{pe} = (4\pi e^2 n_b/m_0)^{1/2}$ is the beam plasma frequency, and γ and $V_\parallel$ are the electron relativistic factor and the axial velocity, respectively. The perpendicular velocity $V_\perp$ can be obtained in a straightforward way from Eq. (4):

$$V_\perp = \frac{\alpha}{1-\alpha}\sum_{n=1}^{\infty}\frac{V_\parallel(\Omega_0/\gamma V_\parallel)^2 b_n\, I_1(k_n\,R)}{(\Omega_0/\gamma V_\parallel)^2-\omega_{pe}^2/2\gamma^3 V_\parallel^2-k_n^2}\sin(k_n\,z), \tag{5}$$

which together with the energy conservation describes a multiresonance behavior at the harmonics of the rippled field:

$$k_n = n\frac{2\pi}{L} = \left[\left(\frac{\Omega_0}{\gamma V_\parallel}\right)^2-\frac{\omega_{pe}}{2\gamma^3 V_\parallel^2}\right]^{1/2}. \tag{6}$$

Conversion of an axial energy into a transverse motion can be achieved by adjusting the electron beam parameters to satisfy the resonance condition Eq. (6) for one of the undulator harmonics.

The electron behavior in an asymmetric undulator has been analyzed numerically with a particle simulation code.[8] Figure 1 represents the electron trajectories in a 40-mm fundamental period undulator, with a large second harmonic components of 20-mm period. The effect of the second harmonics on the electron trajectories can be seen clearly. The average $\langle V_\perp/V_\parallel\rangle$ over the entire beam radius reaches 0.21 near the resonance magnetic field, Fig. 2. The interaction with the asymmetric undulator can transfer the electron kinetic energy into coherent electromagnetic radiation via the

[a)] Permanent address: Applied Physics Dept., Ministry of Defense, P. O. Box 2250, Haifa, Israel.

 0003-6951/85/100936-03$01.00

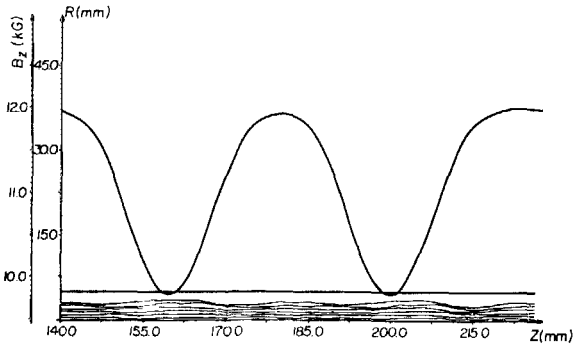

FIG. 1. Computer simulation of electron trajectories at $B_z = 12$ kG. The undulator period is 40 mm. The influence of the second harmonic of the rippled magnetic field on the electron orbit can be observed.

free-electron laser[9] or the cyclotron maser instabilities.[6]

In this letter we represent the experimental results of microwave radiation in the relativistic cyclotron maser mode. The dispersion relations consist of the waveguide dispersion relation together with the Doppler shifted cyclotron wave:

$$\omega^2 - k^2c^2 - \omega_c^2 = 0\,, \tag{7}$$

$$\omega - kV_{\parallel} - \Omega_0/\gamma = 0\,, \tag{8}$$

where ω_c is the waveguide cut-off frequency for the amplified mode. The temporal growth rate is given by

$$\Gamma \simeq \frac{3}{2}\left(\frac{\omega_{pe}^2}{2\gamma}\frac{\Omega_0^2}{\omega\gamma^2}(XJ_1'(X))^2\right)^{1/3}, \tag{9}$$

where $X \equiv \beta_\perp \omega_c/(\Omega_0/\gamma)$. In this mode of operation the high harmonics of the asymmetric undulator affect the temporal growth rate Eq. (9), via $\beta_\perp$ through Eq. (5). The dispersion relation for the free-electron laser case can be written[10]:

$$\omega - (k + k_n)V_{\parallel} - \Omega_0/\gamma = 0\,, \tag{10}$$

where the higher harmonics of the undulator k_n enable operation at higher frequencies. The amplification is expected for ω and k near the simultaneous zeroes of (10) and (7).

The experimental setup[11] consists of a 750-kV, 12-kA, 10-ns electron beam accelerator (PI 105), energizing a foilless diode with a 50-mm-diam spherical graphite cathode. A 1.0-kA beam is extracted through a 6-mm-diam aperture of

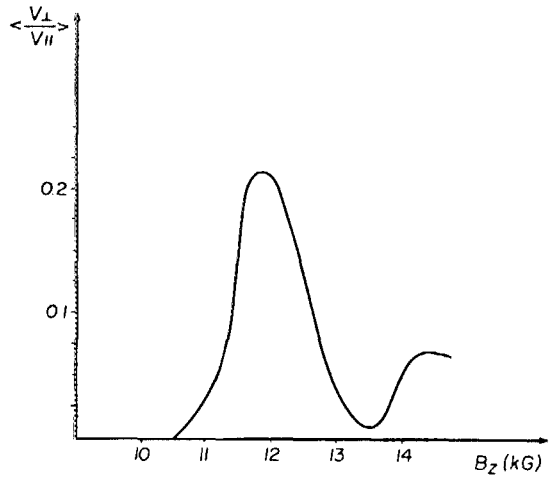

FIG. 2. Simulated distribution $\langle V_\perp/V_\parallel \rangle$ vs axial magnetic field near the resonance. 40-mm period undulator.

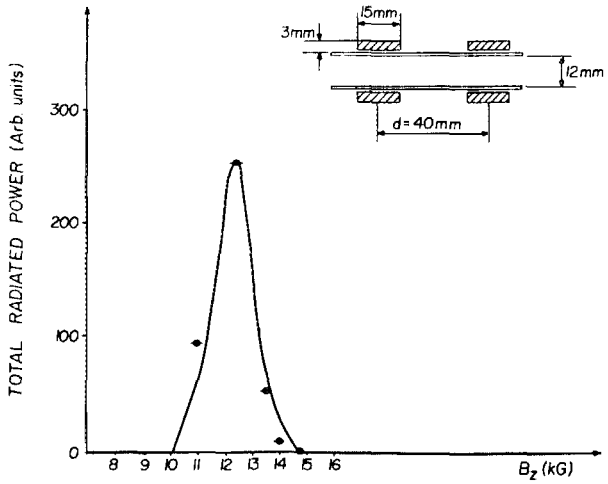

FIG. 3. Total radiated power vs axial magnetic field using 40-mm asymmetric period undulator.

the plane graphite anode and launched into an 11-mm i.d., 500-mm-long stainless steel drift tube. The diode is immersed in uniform pulsed axial magnetic field with 200-μs rise time.

Periodic perturbations in the magnetic field were accomplished by alternating aluminium and lucite rings. The aluminium ring thickness was changed gradually to assure adiabatic change of the radial magnetic field.

The microwaves are radiated via a conical horn antenna placed at the end of the drift tube and terminated by a quartz window which provides the vacuum sealing. The microwave frequency spectrum is measured by a grating spectrometer, in the range of 60–140 GHz. A typical dependence of the total radiated power as a function of the uniform axial magnetic field in the presence of a 40-mm asymmetric undulator is shown in Fig. 3. The configuration of this undulator has a large second harmonic component of the 20-mm period. The maximum microwave power has been detected at $B_0 = 12.5$ kG while the maximum at the fundamental period is expected, according to Eq. (6), at 5.8 kG. The sharp peak of 2 kG full width at half-maximum is expected at the undulator second harmonic resonance. The spectral distribution of the microwave radiation is depicted in Fig. 4, with a maximum at 80 ± 5 and 120 ± 5 GHz. Those frequencies fit with the intersections calculated from Eqs. (7) and (8) for the TE_{01}

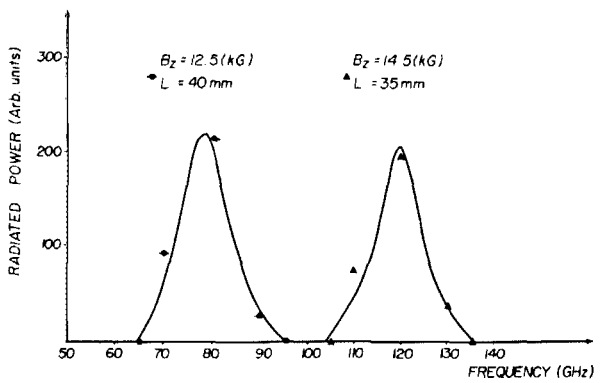

FIG. 4. Spectrum in the 60–140-GHz frequency range measured with a millimeter wave grating spectrometer using a 40-mm and 35-mm asymmetric period undulator B_z = 12.5 kG and 14.5 kG, respectively.

waveguide mode. For the same configuration, assuming free-electron laser mechanism, the expected frequencies [calculated from (7) and (10) for $n = 2$ and TE_{01}] are 235 and 280 GHz, respectively. It should be noted that the maximum microwave radiated power is achieved at a magnetic field slightly higher than the value which corresponds to the dip observed in the electron current. The microwave radiation using magnetic undulator of 47-mm fundamental period was also investigated. Again, the effect of the second harmonic of the rippled field on the microwave emission has been observed.

In summary, we have presented the effect of an asymmetric undulator on the cyclotron maser radiation. The influence of the second harmonic of the rippled magnetic field was investigated numerically and experimentally. The microwave frequencies were found to fit the dispersion relations of the cyclotron maser and TE_{01} mode. The use of the second harmonic of the undulator in a free-electron laser mode may enable higher frequency generation in such a free-electron laser.

[1]P. Sprangle, R. A. Smith, and V. L. Granatstein, in *Infrared and Millimeter Waves*, edited by K. J. Batton (Academic, NY, 1979), Vol. 1, p. 279.
[2]J. L. Hirshfield and V. L. Granatstein, IEEE Trans. Microwave Theory Tech. **25**, 522 (1977).
[3]S. Talmadge, T. C. Marshall, and S. P. Schlesinger, Phys. Fluids **20**, 974 (1977).
[4]R. E. Shefer and G. Bekefi, Int. J. Electron **51**, 569 (1981).
[5]E. Ott and W. M. Manheimer, IEEE Trans. Plasma. Sci. **PS-3**, 1 (1974).
[6]H. S. Uhm and R. C. Davidson, J. Appl. Phys. **50**, 696 (1979).
[7]P. Sprangle and V. L. Granatstein, Phys. Rev. **17**, 1792 (1978).
[8]W. B. Hermansfeld, Stanford Report No. SLAC-166, 1973.
[9]R. C. Davidson and W. A. McMullin, Phys. Fluids **26**, 840 (1983).
[10]A. A. Grossman, Ph. D. thesis, Columbia University, NY 1982 (unpublished).
[11]I. Shraga, Y. Goren, Ch. Leibovitch, S. Eckhouse, and A. Gover, in *Beam 83: Proceedings of the Fifth International Conference on High-Power Particle Beams*, edited by R. J. Briggs and A. J. Toepfer, Sep. 1983, San Francisco, CA.

Optogalvanic study of excited H atoms in a dc glow discharge

Randy D. May
Department of Chemistry, University of North Carolina, Chapel Hill, North Carolina 27514

(Received 8 January 1985; accepted for publication 1 March 1985)

A cw dye laser operating at 6563 Å has been used to measure Doppler broadened absorption profiles of atomic hydrogen in a glow discharge using optogalvanic detection. In the cathode fall region, neutral hydrogen atoms were observed having kinetic energies > 140 eV. In the negative glow and positive column average kinetic energies correspond more nearly to thermal velocities.

Low pressure discharges in neon-containing trace amounts of hydrogen-containing species, primarily H_2, were found to contain a large concentration of excited hydrogen atoms. From a measurement of the spatially resolved Doppler broadened linewidth, the average kinetic energy of $H^*(n = 2)$ atoms in various discharge regions was determined. In the present experiment kinetic energy values exceeding 140 eV were observed in the cathode fall region and can be attributed to the formation of high velocity H atoms by backscattering-neutralization processes at the cathode surface. Much higher H^* concentrations were found in the positive column and are proposed to arise from the efficiency of dissociative processes in this region. These results are consistent with recent interpretations of the H_α emission line shape in H_2 and H_2/He discharges.[1]

Two different discharge cells were used for the optogalvanic (OG) measurements. For transverse excitation in the cathode fall region a parallel plate configuration was constructed having 1.0-cm-diam stainless steel electrodes spaced by 1.4 cm. For transverse excitation in the positive column, and for axial absorption studies, cylindrical stainless steel electrodes (2.0 cm length $\times$ 0.8 cm o.d.) were situated 10.0 cm apart in a water-cooled Pyrex tube (1.0 cm i.d.). A series resistance of 10 kΩ provided stable discharge operation at neon pressures of 0.5–15 Torr and currents of 1–70 mA. OG signals were extracted from the high voltage anode via a 0.01-μF capacitor and either processed by a lock-in amplifier or displayed on an oscilloscope. A mechanical chopper modulated the beam from a dye laser (CR 595) at 400 Hz and served as a reference for the lock-in detector. Laser dye DCM provided up to 300 mW multimode when pumped by 2.5 W from an all-line argon ion laser. A pair of solid etalons ($d = 1$ cm, $d = 0.1$ cm) could be inserted into the laser cavity for single frequency operation. Scan rates and frequency calibration were determined from a calibration of the laser wavelength drive using the neon OG spectrum.[2] A background pressure of 5×10^{-6} Torr was maintained in the discharge cell using a liquid nitrogen trapped diffusion pump system. The research grade neon (99.999%) had a stated H_2 impurity level of 2 ppm or densities of $\sim 3 \times 10^{10}$–1×10^{12} cm^{-3} at the pressures used. Other possible sources of hydrogen in the neon gas were CH_4 (~ 0.1 ppm) and H_2O (~ 2 ppm) that were not effectively removed by the traps.

Typical OG line profiles are shown in Fig. 1 for transverse excitation in the cathode fall, negative glow, and posi-

0003-6951/85/100938-03$01.00